

Ability to Induce Atrial Fibrillation in the Peri-operative Period Is Associated with Phosphorylation-dependent Inhibition of TWIK Protein-related Acid-sensitive Potassium Channel 1 (TASK-1)*

[Erin Harleton](#),[‡] [Alessandra Besana](#),[‡] [George M. Comas](#),[§] [Peter Danilo, Jr.](#),[‡] [Tove S. Rosen](#),[¶] [Michael Argenziano](#),[§] [Michael R. Rosen](#),^{‡¶||} [Richard B. Robinson](#),^{‡||} and [Steven J. Feinmark](#)^{‡||,1}

From the Departments of [‡]Pharmacology,

[§]Surgery, and

[¶]Pediatrics and

the ^{||}Center for Molecular Therapeutics, Columbia University Medical Center, New York, New York 10032

¹ To whom correspondence should be addressed: Dept. of Pharmacology, Columbia University Medical Center, 630 W. 168th St., New York, NY 10032., Tel.: Phone: 212-305-3567; Fax: 212-305-4741; E-mail: sjf1@columbia.edu.

Received 2012 Jul 26; Revised 2012 Nov 21

Copyright © 2013 by The American Society for Biochemistry and Molecular Biology, Inc.

Abstract

Peri-operative atrial fibrillation (peri-op AF) is a common complication following thoracic surgery. This arrhythmia is thought to be triggered by an inflammatory response and can be reproduced in various animal models. Previous work has shown that the lipid inflammatory mediator, platelet-activating factor (PAF), synthesized by activated neutrophils, can induce atrial and ventricular arrhythmias as well as repolarization abnormalities in isolated ventricular myocytes. We have previously shown that carbamylated PAF-induced repolarization abnormalities result from the protein kinase C (PKC) ϵ -dependent phosphorylation of the two-pore domain potassium channel TASK-1. We now demonstrate that canine peri-op AF is associated with the phosphorylation-dependent loss of TASK-1 current. Further studies identified threonine 383 in the C terminus of human and canine TASK-1 as the phosphorylation site required for PAF-dependent inhibition of the channel. Using a novel phosphorylation site-specific antibody targeting the phosphorylated channel, we have determined that peri-op AF is associated with the loss of TASK-1 current and increased phosphorylation of TASK-1 at this site.

Keywords: Electrophysiology, Heart, Patch Clamp Electrophysiology, Potassium Channels, Protein Kinase C (PKC), TASK-1, Atrial Fibrillation, Platelet-activating Factor, Two-pore Domain Potassium Channel

Introduction

Atrial fibrillation (AF),² the most common sustained arrhythmia in humans, can lead to an increased risk of stroke and other morbidities. Although AF may have many underlying causes, one particular form occurs commonly in the peri-operative period after thoracic surgery (peri-op AF), affecting as many as 60% of patients within 2–3 days of surgery (1). Inflammation is thought to contribute to the etiology of this disease, with the peak incidence of peri-op AF coinciding with the peak levels of circulating C reactive protein, interleukins-1 and -6, complement components, and leukocytes (2). Activation of neutrophils alone is known to be arrhythmogenic (3, 4), and one of the neutrophil products that contributes

to arrhythmogenicity is the inflammatory lipid mediator, platelet-activating factor (PAF) (5). Myocytes express the PAF receptor that, when activated, leads to the activation of a downstream kinase, which we have shown targets the two-pore domain K⁺ channel (K_{2P}) TASK-1, resulting in inhibition of the channel (6, 7). Our current results suggest that the loss of the TASK-1 current may contribute to the arrhythmogenic effect of PAF.

The two-pore domain potassium channels are a recently characterized family of K⁺-selective channels. They are neither voltage-gated nor time-dependent and carry background or “leak” currents that help set the membrane potential and contribute to membrane repolarization. There is an expanding body of work describing the importance of these channels in the cardiovascular system (8). Unlike other K⁺ channel families, K_{2P} forms functional dimers. Each subunit is composed of four membrane-spanning units, two pore-forming units, a relatively short cytoplasmic N-terminal tail, and a longer C-terminal tail. The C terminus contains numerous regulatory sites, including phosphorylation sites and the putative lipid-binding domain (9, 10). These channels are generally insensitive to common K⁺ channel blockers such as TEA, 4-aminopyridine, and Ba²⁺, and this property can be used to pharmacologically isolate K_{2P} currents from other potassium currents in native tissues, which may contain numerous K⁺-selective channels. TASK-1 is an openly rectifying channel with a current-voltage relation that is linear in the presence of symmetrical K⁺ and outwardly rectifying in physiological solution. It is blocked by the endocannabinoid anandamide and its nonhydrolyzable analog, methanandamide (11). Methanandamide inhibition provides a means to measure basal TASK-1 current in cells by calculating the difference in current before and after treatment with the drug.

TASK-1-deficient transgenic mice have a mild cardiac phenotype, with a faster resting heart rate, a longer rate-corrected QT interval, and a broader QRS complex (12, 13) than wild-type mice, suggesting a role for TASK-1 in excitability and in ventricular repolarization in rodents. In human atrial myocytes, TASK-1 inhibition leads to action potential prolongation (14), indicating that TASK-1 may have an important function in the human atrial action potential.

In studies of isolated murine ventricular myocytes, we have shown that PAF elicits repolarization abnormalities via PKCε-dependent inhibition of TASK-1 (7), indicating that TASK-1 phosphorylation may be a potential therapeutic target in arrhythmias with an inflammatory component. To elucidate the connection between inflammation, TASK-1 inhibition, and arrhythmogenesis, we have implemented a canine model of peri-operative AF to characterize the regulation and functional role of TASK-1 in the atrium.

EXPERIMENTAL PROCEDURES

Peri-operative AF Model This study was performed under a protocol approved by the Institutional Animal Care and Use Committee of Columbia University, according to a modification of the method described by Ishii *et al.* (15). Briefly, a thoracotomy was performed on anesthetized adult male mongrel canines (25–35 kg) treated with thiopental sodium (17 mg/kg i.v.) and ventilated with isoflurane (1.5–2%) and O₂ (2 liters/min). A 5-cm right atriotomy was performed, and atrial tissue was collected into cold saline for processing and analysis. Electrical leads were placed on the high and mid-right atrium for recording and low right atrium for pacing. The chest was closed, and the animals were allowed to recover with appropriate pain management. Three days later, the animals were reanesthetized, the chest reopened, and the heart subjected to 30-s bursts of pacing at decreasing cycle lengths (starting at 30 ms above the effective refractory period) until atrial fibrillation was induced or a cycle length of 50 ms was reached. If this pacing protocol did not induce AF, the dog was allowed to rest 30 min before another attempt. If AF was induced, the arrhythmia was allowed to continue until it spontaneously converted to normal sinus

rhythm or for 30 min, at which time the heart was electrically cardioverted. The experiment continued for up to 5 h after the first induction attempt or until there were three consecutive unsuccessful induction attempts. At the end of the protocol, a cardiectomy was performed, and the atrium was dissected and collected into cold saline for processing and analysis. Further analyses were performed on relatively healthy tissue adjacent to the atriotomy scar. Thirty five animals were used for this study, of which 24 developed AF (69%) and 11 did not (referred to as failed AF dogs). Because of the limited amount of atrial tissue resulting from each surgery, not all analyses were carried out on every animal.

Myocyte Isolation Tissue was diced in physiological solution (composition in mM: NaCl 140, KCl 5.4, HEPES 5, NaOH 2.3, glucose 10, CaCl₂ 1, MgCl₂ 1, pH 7.4) and then rinsed in Ca²⁺-free solution (composition in mM: NaCl 140, KCl 5.4, HEPES 5, MgCl₂ 0.5, KH₂PO₄ 1.2, glucose 5.5, taurine 50, pH 6.9). Next, the pieces were incubated in an enzyme solution and bubbled with O₂ at 37 °C. The enzyme solution was made by adding collagenase (59.4 units/ml; Worthington CLS2, 198 units/mg) and protease (0.52 units/ml; Sigma type XIV, 5.2 units/mg) to the Ca²⁺-free solution. 45–60 min after the initial exposure of the tissue to the enzymes and every 10–15 min thereafter, the supernatant was checked for the appearance of myocytes. If myocytes were present, the supernatant was centrifuged and the pellet was resuspended in Ca²⁺-free physiological solution and then slowly adapted to a physiological Ca²⁺ concentration (1 mM). Only the rod-shaped and striated myocytes were used for electrophysiological studies.

Electrophysiological Recordings in Myocytes TASK-1 current was measured in whole cell configuration using a ramp protocol from –50 to +30 mV over 6 s. The cells were superfused at room temperature with a modified Tyrode's solution to minimize other K⁺ currents and to reduce the outward rectification of TASK-1 (composition in mM: NaCl 100, KCl 50, CaCl₂ 1, MgCl₂ 1, HEPES 5, glucose 10, CsCl 5, TEA 2, and nifedipine 5 μM). Borosilicate glass pipettes with a tip resistance between 3 and 5 megohms were used. Pipettes were filled with a solution containing (in mM) aspartic acid 130, KOH 146, NaCl 10, CaCl₂ 2, EGTA 5, HEPES 10, MgATP 2, adjusted to pH 7.2. The recordings were made using an Axopatch 200B amplifier and a Digidata 1200 interface. TASK-1 current was measured as the methanandamide-sensitive difference current (10 μM). In recordings with PP2A, the tip of the pipette was filled with the phosphatase (1 unit/ml) and then backfilled with regular pipette solution. The recordings started 10–12 min after rupture to allow the PP2A to dialyze into the cell.

Electrophysiological Recordings in CHO Cells The full-length human TASK-1 gene (NCBI accession number [NM_002246.2](#)) was subcloned into a pDC-IE vector, which co-expresses GFP, and mutations were made in putative phosphorylation sites using the PCR-based QuikChange kit (Agilent) substituting alanine for threonine or serine residues. CHO cells were transfected with the wild-type or mutant constructs using GeneJammer (Agilent). After 48 h, cells were checked for green fluorescence and then plated and superfused at room temperature with a Tyrode's solution (composition in mM: NaCl 140, KCl 5.4, CaCl₂ 1, MgCl₂ 1, HEPES 5, glucose 10, adjusted to pH 7.4). The current was recorded using a voltage clamp protocol (ramp from –110 to +30 mV in 6 s) in whole cell configuration using borosilicate glass pipettes with a tip resistance between 4 and 6 megohms and filled with a solution containing (in mM) aspartic acid 130, KOH 146, NaCl 10, CaCl₂ 2, EGTA 5, HEPES 10, MgATP 2, adjusted to pH 7.2. In recordings with C-PAF, the lipid was dissolved in water and diluted in external recording solution to a final concentration of 185 nM. In recordings with the PKCε inhibitor peptide or scrambled control peptide, peptides were diluted in pipette solution and added to the patch pipette tip as above.

All protocols were generated using Clampex 8 software. Steady state traces were acquired at 500 Hz analog, filtered at 1 KHz (lowpass Bessel filter). Currents are expressed as current densities, after normalizing to cell capacitance. All of the recordings were performed at room temperature and have been

corrected for the junction potential (−9.8 mV).

Myeloperoxidase Assay Atrial tissue was frozen after collection and was prepared and analyzed using a modification of Bradley *et al.* (16). Tissue was thawed, minced, and homogenized in 50 mM KPO₄ buffer, pH 6.0, containing 0.5% hexadecyltrimethylammonium bromide. The homogenate was sonicated for 10 s, freeze-thawed in a dry ice acetone bath, sonicated an additional 10 s, and centrifuged at 40,000 × *g*. Samples were read in duplicate in a 96-well plate format, combining supernatant (6.7 μl) with KPO₄ (pH 6; 193 μl) containing *o*-dianisidine dihydrochloride (0.167 mg/ml) and 0.0005% H₂O₂. The increase in absorbance at 450 nm was measured 10 times in 10-s increments using an EL312 plate reader (Biotek). The slope of this change in absorbance was compared with that of a standard curve of purified human leukocyte myeloperoxidase enzyme (0.01–3 units/ml serial dilutions, in triplicate; Axxora).

Fusion Constructs and in Vitro Kinase Assay The distal 45 residues of the C terminus of human TASK-1 were fused with glutathione *S*-transferase using the pGEX4T3 vector (GE Healthcare), and site-directed mutations were made in the putative phosphorylation sites using the PCR-based QuikChange kit (Agilent). GST/hTASK-1 C-terminal constructs were expressed in BL-21 Gold *Escherichia coli* cells (Agilent), purified using the B-PER GST fusion protein purification kit (Pierce), and concentrated by ultrafiltration in Vivaspin columns.

Purified fusion proteins were phosphorylated by recombinant PKCε (25 μg of PKCε/μg of substrate) in the presence of [γ -³²P]ATP (3 μCi/66 μM) and were resolved by SDS-PAGE, blotted to nitrocellulose, and exposed to x-ray film. In parallel experiments, fusion protein was phosphorylated, digested with trypsin, and analyzed by LC/MS/MS to determine the phosphorylation site.

Treatment of Canine Atrium with C-PAF Right atrial tissue was taken from control dogs and minced. 50–200 mg of tissue was incubated in Tyrode's solution (2 ml) supplemented with NaF (1 mM). Reactions were bubbled with O₂, and C-PAF (0–2 μM) was added for 15 min of incubation at 37 °C. In some reactions, the PKC inhibitor bisindolylmaleimide I (BIM-1; 5 μM) was added to the tissue incubations before the addition of C-PAF. Tissue was removed from the incubation bath and frozen. Samples were processed and immunoblotted as described below.

Immunoblotting A phosphorylation site-specific antibody was raised in rabbits against residues 376–389 of human (h) TASK-1 and phosphorylated at Thr-383 (Yenzyme). Specificity of the antibody was validated by running 500 ng of purified wild-type or T383A GST/hTASK-1 C-terminal construct, with or without PKCε phosphorylation, or 500 ng of phosphorylated construct before or after treatment with acid phosphatase (Sigma; 1.1 units) on a 12.5% SDS-polyacrylamide gel, and transferring to nitrocellulose according to standard protocols. The phosphorylated TASK-1 band was visualized by incubation with the phosphorylation site-specific antibody (10 μg/ml) followed by incubation with a sheep anti-rabbit antibody coupled to horseradish peroxidase (GE Healthcare), development with PicoWest ECL substrate (Pierce), and exposure to x-ray film. Equal loading of fusion proteins was verified by immunoblotting against GST (0.04 μg/ml; Santa Cruz Biotechnology) in parallel.

Atrial tissue was frozen after collection and then separated into crude membrane and cytosolic fractions by standard methods. Briefly, tissue was thawed, minced, and homogenized in a detergent-free homogenization buffer (composition in mM: Tris-HCl 50, NaCl 150, EGTA 1, sucrose 250, sodium orthovanadate 5, NaF 5, PMSF 0.1, 1 ng/ml apoprotinin, 1 ng/ml leupeptin, pepstatin 0.0001, 1 μg/ml benzamidine, adjusted to pH 7.4). After removing debris by centrifugation at 3000 × *g*, the homogenate was centrifuged at 160,000 × *g*, and the resulting pellet was resuspended in homogenization buffer containing 1% Triton X-100, resulting in a crude membrane preparation. Total protein concentration was determined by a modification of the method of Lowry (17). 30 μg of total protein from each sample was

loaded into duplicate lanes, run onto 10% polyacrylamide Tris-glycine gels, and transferred to nitrocellulose membranes according to standard protocols. The phosphorylated TASK-1 band and total TASK-1 were visualized by incubation with the custom phosphorylation site-specific antibody (10 µg/ml) or with a rabbit polyclonal antibody raised against the ²⁵²EDEKRDAEHRALLTRNGQ²⁶⁹ epitope of the hTASK1 protein (1.4 µg/ml; Biomol) followed by incubation with a sheep anti-rabbit antibody coupled to horseradish peroxidase (GE Healthcare), development with PicoWest ECL substrate (Pierce), and exposure to x-ray film. Films were scanned, and band intensity was measured using ImageJ software (National Institutes of Health).

Drugs Methanandamide (Biomol) was prepared as a stock solution in DMSO and then diluted to its final concentration in the external recording solution (final DMSO <0.1%). A stock solution of PP2A (Millipore) was prepared in a buffer solution (provided by the manufacturer) and then diluted to the final concentration of 1 unit/ml in the pipette solution. C-PAF (Biomol) was dissolved in water (25 µg/µl), and the stock solution was diluted to 185 nM in external recording solution. BIM-1 (Sigma) was dissolved in DMSO and diluted to 5 mM in incubation buffer prior to use (final DMSO <0.1%). The specific PKCε-inhibitor peptide and a scrambled control peptide (7, 18) were synthesized by the Columbia University Medical Center Protein Core facility and were prepared in water and then diluted to the final concentration of 100 nM in pipette solution.

Data Analysis and Statistics Electrophysiological data were analyzed using pCLAMP 8.0 (Axon) and Origin 7.0 (Microcal) and are presented as mean ± S.E. For each myocyte, TASK-1 current was obtained as the difference between the average of the traces at steady state under control conditions and in the presence of methanandamide. Student's *t* test and analysis of variance (with Bonferroni's multiple comparisons tests) were used to compare data; a value of *p* < 0.05 was considered statistically significant.

RESULTS

Peri-operative AF Is Associated with Neutrophil Influx and Phosphorylation-dependent Loss of TASK-1 Current

Peri-operative AF was induced in canines by rapid pacing 3 days after a right atriotomy that created a structural and inflammatory insult. Significant inflammation was quantified by comparing the presence of neutrophils as measured by the neutrophil-specific enzyme, myeloperoxidase, in the right atrium before and after induction of AF (1.0 ± 0.2 unit/g in control tissue *versus* 36.8 ± 4.8 units/g after AF; *n* = 17; *p* < 0.001). These results are similar to those observed by Ishii *et al.* (15). In tissue from failed AF animals, myeloperoxidase levels were intermediate (19.5 ± 4.3 units/g; *n* = 11), significantly greater than preoperative control tissue (*p* < 0.001) but significantly less than tissue from dogs in which AF induction was successful (*p* < 0.05).

Our previous *in vitro* data suggested that inflammatory lipids could induce phosphorylation and inhibition of the K_{2P} channel TASK-1, which might play a role in arrhythmogenesis. Therefore, we measured TASK-1 current levels in atrial myocytes isolated from animals before and after induction of peri-operative AF. Patch clamp recording was used to measure TASK-1 current in myocytes isolated from the section of right atrial free wall that was excised in the initial atriotomy procedure, before and after the addition of the TASK-1 inhibitor methanandamide (Fig. 1A). From these observations, we calculated a methanandamide-sensitive difference current that was taken to be TASK-1 (Fig. 1B). The average methanandamide-sensitive TASK-1 current from control myocytes was 0.47 ± 0.10 pA/pF at +30 mV (Fig. 2A, filled circles; *n* = 52 cells from 21 dogs).

After the surgical and pacing protocols, we measured TASK-1 current in right atrial tissue adjacent to the atriotomy scar. In myocytes from dogs with peri-op AF, TASK-1 current was absent (Fig. 2B, filled circles), averaging -0.02 ± 0.08 pA/pF at +30 mV (*n* = 19 cells from seven dogs; *p* < 0.0001 *versus*

pre-operative control). TASK-1 current in cells from dogs with failed AF was not significantly different from levels seen in cells from preoperative control tissue (Fig. 2C; 0.44 ± 0.20 pA/pF; $n = 12$ cells from four dogs).

Because we had previously shown that the murine TASK-1 channel is inhibited after phosphorylation by PKC ϵ (7), we asked whether canine myocyte TASK-1 was also inhibited in a phosphorylation-dependent manner. We treated cells intracellularly with the serine/threonine phosphatase PP2A and allowed the phosphatase to dialyze into cells isolated from peri-op AF dogs. In these cells, TASK-1 current was rescued (Fig. 2B, open circles), averaging 0.27 ± 0.05 pA/pF at +30 mV ($n = 16$ cells from seven dogs; $p > 0.05$ versus preoperative control). PP2A treatment had no effect on TASK-1 current levels in cells from control atrium (Fig. 2A, open circles), averaging 0.36 ± 0.05 pA/pF ($n = 50$ cells from 20 dogs) or on cells from failed AF dogs (0.22 ± 0.08 pA/pF, $n = 5$ cells from two dogs).

Thr-383 Is an Inhibitory PKC ϵ Phosphorylation Site in the TASK-1 C Terminus C-PAF, a nonhydrolyzable analog of the lipid inflammatory mediator, PAF, inhibits mouse TASK-1 in a PKC ϵ -dependent manner by stimulating the phosphorylation of threonine 381 (Thr-381) in the murine TASK-1 C terminus (7). Therefore, we asked whether PKC ϵ directly phosphorylates canine TASK-1, and if this phosphorylation event is also associated with the loss of TASK-1 current in our peri-operative AF model.

As a first step, we sought to determine the PKC ϵ phosphorylation site in canine TASK-1. Canine TASK-1 and hTASK-1 C termini share significant sequence homology but differ from the mouse sequence in important ways. Specifically, the phosphorylation site in the murine channel is absent in the human and canine sequences. Instead, that region of the canine TASK-1/hTASK-1 C terminus contains two putative PKC phosphorylation sites, identified by homology searches, at serine 358 (Ser-358) and threonine 383 (Thr-383). To determine whether either of these sites were a direct target of PKC ϵ phosphorylation, we made constructs in which the distal 45 amino acids of hTASK-1 were fused to glutathione *S*-transferase (GST). Mutations were then made at each of the putative phosphorylation sites, converting the serine or threonine to a nonphosphorylatable residue, in this case alanine. We then measured the ability of recombinant PKC ϵ to phosphorylate the purified TASK-1 C terminus/GST fusion proteins in the presence of [γ - 32 P]ATP. PKC ϵ catalyzed the incorporation of 32 P into the wild-type C-terminal construct and into the S358A mutant. Label was not incorporated into GST alone or the Thr-383A mutant (Fig. 3), demonstrating that this threonine was necessary for phosphorylation by PKC ϵ . LC/MS/MS analysis of the PKC ϵ -phosphorylated wild-type C-terminal construct confirmed direct phosphorylation at Thr-383 (data not shown).

To determine the possible functional consequence of Thr-383 phosphorylation, we made the same mutations in the full-length hTASK-1 sequence and measured total and C-PAF-sensitive currents by patch clamp recording. Both mutant channels expressed normally and carried a current that was similar in amplitude to wild-type hTASK-1 under control conditions (data not shown). There were, however, striking differences in the way the mutants responded to PKC ϵ activation after treatment of the cells with C-PAF. Fig. 4A shows a typical recording of hTASK-1 current in control conditions and in the presence of C-PAF (187 nM, 5 min perfusion). C-PAF significantly inhibits the current (29 ± 6.3 pA/pF in control and 25.5 ± 5.6 pA/pF after C-PAF; $n = 21$, $p < 0.0001$). The S358A mutation had no effect on the C-PAF-sensitive current, but mutation of threonine 383 to alanine completely ablated the C-PAF effect (Fig. 4B; $p < 0.01$). To verify the requirement for PKC ϵ in the C-PAF-induced inhibition of the TASK-1 current, in agreement with previous observations in the murine channel, a specific PKC ϵ -inhibitor peptide was used (7, 18). Addition of this peptide but not a scrambled control peptide to the patch pipette (100 nM) blocked the effect of C-PAF on all previously responsive forms of the channel (Fig. 4C; $p < 0.05$).

Thr-383 Is Phosphorylated Downstream of C-PAF Signaling After identifying the PKC ϵ phosphorylation site, we

raised an antibody specific for TASK-1 phosphorylated at Thr-383 (Thr(P)-383-TASK-1) to quantify phosphorylation at this site. Characterization of this antibody verified that it recognizes TASK-1 only when Thr-383 is phosphorylated but not the nonphosphorylated form (Fig. 5).

To determine whether Thr-383 phosphorylation changed after native myocardium was exposed to PAF, normal canine atrium was minced and incubated with C-PAF (0–2 μ M). The tissue was then homogenized, and proteins were separated by SDS-PAGE and immunoblotted for total TASK-1 and Thr(P)-383-TASK-1 (Fig. 6A). Changes in the fraction of channels that were phosphorylated were expressed as a ratio of Thr(P)-383-TASK-1 to total TASK-1 signal. After 15 min in the presence of C-PAF (2 μ M), there was a 2.5 ± 0.5 -fold increase in the relative Thr(P)-383-TASK-1 signal (Fig. 6B; $p < 0.05$, $n = 6$). In a separate series of experiments, the PKC dependence of the C-PAF-induced phosphorylation at Thr-383 was tested by incubation of the tissue with the general PKC inhibitor BIM-1. PKC inhibition prevented the C-PAF-dependent phosphorylation of TASK-1 at Thr-383 (Fig. 6C; $p < 0.01$, $n = 6$).

Peri-operative AF Is Associated with Thr-383 Phosphorylation Because an inflammatory mediator induced phosphorylation of TASK-1 at Thr-383, we tested whether the same phosphorylation leads to the loss of TASK-1 current in peri-operative AF, which is clearly an inflammatory event. Using the phosphorylation site-specific antibody, we measured the ratio of Thr(P)-383-TASK-1 to total TASK-1 in membrane homogenates from canine right atrium before and after atriotomy and the induction of AF (Fig. 7A). Interestingly, we observed a significant decrease in total TASK-1 signal after AF induction. The average pixel density fell from 8797 ± 829 to 3792 ± 1063 ($n = 10$; $p < 0.005$). In the face of this decrease in total TASK-1 signal, there was a large and significant increase in Thr(P)-383-TASK-1 signal. The average pixel density rose from 3507 ± 823 to $10,452 \pm 1161$ after induction of peri-operative AF ($n = 10$; $p < 0.001$). Because of the inter-animal variability in TASK-1 signal, data for total TASK-1 and Thr(P)-383 TASK-1 expression were plotted separately for each animal before and after surgery, to better understand the pattern of changes in expression levels (Fig. 7B). The total TASK-1 signal decreased after peri-op AF in 6 of 10 dogs. Even with this decrease in total TASK-1, phosphorylation at Thr-383 increased after peri-op AF in 9 of 10 dogs. To quantify this Thr-383 phosphorylation as a fraction of the total channel, the Thr(P)-383/total TASK-1 ratio was calculated before and after induction of peri-op AF. The Thr(P)-383-TASK-1/total TASK-1 ratio increased from 0.42 ± 0.09 to 5.92 ± 2.07 after AF induction ($n = 10$; $p < 0.05$), roughly a 14-fold increase (Fig. 7C) confirming that the phosphorylation-dependent loss of TASK-1 current in peri-operative AF is associated with a large increase in phosphorylation at Thr-383.

DISCUSSION

Our data show that TASK-1 is inhibited by a PKC ϵ -mediated phosphorylation at threonine 383 in the C-terminal tail. Using a phosphorylation site-specific antibody, we further show that this phosphorylation occurs in native atrial tissue *ex vivo* when exposed to the inflammatory lipid mediator, platelet-activating factor, and in an *in vivo* model of peri-operative AF in the dog. Somewhat paradoxically, in parallel to the increase in Thr(P)-383-TASK-1, we observed a marked decrease in the relative level of total TASK-1 protein in atrial homogenates after peri-op AF. A portion of the reduction may have been due to the formation of scar tissue at the incision site, which must alter the total protein content of the region. Despite this reduction, however, we found that intracellular phosphatase rescue of TASK-1 in isolated atrial myocytes produced current levels that were similar before and after induction of AF (Fig. 2). Therefore, the decrease in TASK-1 protein observed in atria from animals with peri-op AF must not reflect an actual decrease in the number of channels at the membrane. More likely, the result reflects changes in the recycling of channels from the membrane, but the details of this need to be determined with further experimentation. Moreover, given the relative changes in Thr(P)-383-TASK-1 to total TASK-1, our analysis likely underestimates the abundance of phosphorylated channel in atrial myocytes isolated after

peri-op AF.

These studies have expanded on our previous *in vitro* work, which showed that TASK-1 played a role in inflammation-induced repolarization abnormalities in isolated myocytes (6). It has long been known that activated neutrophils contribute to arrhythmogenicity in isolated hearts, and numerous clinical studies have found a link between inflammatory mediators and arrhythmias. We have described repolarization abnormalities caused by the inflammatory mediator PAF, released from activated neutrophils (5), and we determined that C-PAF elicits these effects *in vitro* via PKC ϵ -dependent inhibition of the TASK-1 channel in murine ventricular myocytes (6) and in heterologous expression systems (7). We have now demonstrated a similar phenomenon in intact canine atrium and associated with peri-op AF in the dog.

Our experiments demonstrate that a phosphorylation-dependent inhibition of TASK-1 is associated with successful induction of AF. In myocytes from the dogs in which AF induction failed, TASK-1 current is equal to control levels. Because both groups of dogs undergo identical surgical and pacing protocols, we can infer that the inhibition of TASK-1 is critically related to the development of the arrhythmia, and it either contributes to the creation of the arrhythmogenic substrate or somehow is a consequence of the induction of the arrhythmia.

Although our electrophysiological results in isolated myocytes are clear, it remains uncertain how the loss of a small background current such as TASK-1 could induce arrhythmias in the intact atrium. Although some evidence supports a role of increased potassium currents in the formation of re-entrant arrhythmias (19), there also is emerging evidence to support a role for potassium channel inhibition in the promotion of AF (20–22). Decreased TASK-1 current could promote the initiation or maintenance of an arrhythmia by prolonging the action potential duration and causing after depolarizations, spurring ectopic beats and inhomogeneity of refractoriness that can lead to re-entry. These phenomena have been studied extensively in the ventricle, including in the TASK-1 knock-out mouse (12, 13) and in mouse and rat ventricular myocytes after TASK-1 inhibition (6, 23). However, the properties of the ventricular action potential differ greatly from the atrial action potential, and thus an alternative mechanism may be at work in this model of peri-op AF.

Two potential limitations of our study design are noted. First, we have not included dogs that underwent the surgical protocol but were not paced, nor have we included dogs that were paced in the absence of surgery. It is clear from the literature that atriotomy alone, in the absence of burst pacing, is insufficient to induce AF in the dog (15). Also, it is well established that burst pacing alone is insufficient to induce sustained AF in normal canine hearts (24, 25) without some additional hormonal, neuronal, or surgical intervention. Because it is clear that these dogs would not have developed AF and thus would not have contributed results relevant to the major aims of these studies, they were omitted. Therefore, we cannot conclude that the inflammation resulting from the atriotomy alone is sufficient to induce TASK-1 inhibition in the absence of pacing. However, data from the failed AF dogs allow us to conclude that loss of TASK-1 current is critical to the development of AF in this model because normal TASK-1 current was always found in hearts in which AF could not be induced despite the atriotomy. A second potential limitation involves the use of isoflurane as an anesthetic in these surgical procedures. Isoflurane has been shown to activate TASK-1 in single cell recordings (26). Additionally, in the intact canine, isoflurane has been shown to increase the stimulus required to induce AF during electrophysiological pacing (27). The combination of these effects may have increased the difficulty of AF induction in our studies. However, they would have no effect on any of the single cell electrophysiological or biochemical studies completed *ex vivo* or *in vitro*.

Extensive work has been done in various models to elucidate the role of PAF signaling in the promotion of arrhythmias (28). Exogenous PAF caused ventricular tachycardias in Langendorff-perfused rat hearts (29)

and potentiated ischemia-induced arrhythmias in Langendorff-perfused guinea pig hearts (30). In mice, overexpression of the PAF receptor (PAFR) as a transgene resulted in increased sensitivity to PAF-induced arrhythmias (31). Because PAF is present in the inflammatory milieu following coronary ischemia (32), there has been interest in investigating PAFR antagonists as antiarrhythmic agents in ischemia-reperfusion injury. Indeed, PAFR antagonism has been shown to be effective in preventing post-ischemia arrhythmias *ex vivo* (33) and *in vivo* (34, 35). Unfortunately, one PAFR antagonist has been shown to promote QT interval prolongation and coronary vasodilation, resulting in hypotension and arrhythmogenic potential (33). Although these do not appear to be class effects (36), to our knowledge no clinical studies investigating PAFR antagonism as an antiarrhythmic strategy, either peri-operatively or after myocardial infarction, have been attempted.

This work has identified TASK-1 as a physiologically relevant downstream target of inflammation and PAFR signaling. If TASK-1 inhibition indeed contributes to the arrhythmogenic effects of PAF, targeting TASK-1 could provide a more direct way to prevent peri-operative AF with fewer unwanted effects. Therapies aimed at preventing TASK-1 inhibition or restoring this small conductance potassium current could prove to be promising avenues for future *in vivo* work.

Acknowledgments

We thank Mary Ann Gawinowicz in the Columbia University Medical Center Protein Chemistry facility for performing mass spectrometry and Robert Sciacca for advice with statistical analyses.

* This work was supported, in whole or in part, by National Institutes of Health Grants R01 HL70105 (to S. J. F.) and HL67101 (to M. R. R.) from NHLBI and Grant TL1 TR000082 from National Center for Advancing Translational Sciences (formerly NCCR) and Grant TL1 RR024158. This work was also supported by grants from the PhRMA Foundation, Institut de Recherches Servier, and a career development award from the Thoracic Surgery Foundation for Research and Education (to M. A.).

²The abbreviations used are:

AF atrial fibrillation
peri-op AF peri-operative atrial fibrillation
PAF platelet-activating factor
K_{2p} two-pore domain potassium channel
TASK TWIK-related acid-sensitive potassium channel
hTASK human TASK
C-PAF carbamyl-PAF
BIM-1 bisindolylmaleimide I
PP2A protein phosphatase 2A
PAFR platelet-activating factor receptor
TEA tetraethylammonium
pF picofarad.

REFERENCES

1. Hogue C. W., Jr., Creswell L. L., Gutterman D. D., Fleisher L. A. (2005) Epidemiology, mechanisms, and risks. American College of Chest Physicians guidelines for the prevention and management of postoperative atrial fibrillation after cardiac surgery. *Chest* 128, 9S–16S [PubMed: 16167659]
2. Baker W. L., White C. M. (2007) Post-cardiothoracic surgery atrial fibrillation. A review of preventive strategies. *Ann. Pharmacother.* 41, 587–598 [PubMed: 17374620]
3. Hoffman B. F., Feinmark S. J., Guo S. D. (1997) Electrophysiologic effects of interactions between

activated canine neutrophils and cardiac myocytes. *J. Cardiovasc. Electrophysiol.* 8, 679–687 [PubMed: 9209969]

4. Dhein S., Schott M., Gottwald E., Müller A., Klaus W. (1995) The contribution of neutrophils to reperfusion arrhythmias and a possible role for antiadhesive pharmacological substances. *Cardiovasc. Res.* 30, 881–888 [PubMed: 8746202]

5. Hoffman B. F., Guo S. D., Feinmark S. J. (1996) Arrhythmias caused by platelet activating factor. *J. Cardiovasc. Electrophysiol.* 7, 120–133 [PubMed: 8853022]

6. Barbuti A., Ishii S., Shimizu T., Robinson R. B., Feinmark S. J. (2002) Block of the background K^+ channel TASK-1 contributes to arrhythmogenic effects of platelet-activating factor. *Am. J. Physiol. Heart Circ. Physiol.* 282, H2024–H2030 [PubMed: 12003807]

7. Besana A., Barbuti A., Tateyama M. A., Symes A. J., Robinson R. B., Feinmark S. J. (2004) Activation of protein kinase $C\epsilon$ inhibits the two-pore domain K^+ channel, TASK-1, inducing repolarization abnormalities in cardiac ventricular myocytes. *J. Biol. Chem.* 279, 33154–33160 [PubMed: 15184378]

8. Gurney A., Manoury B. (2009) Two-pore potassium channels in the cardiovascular system. *Eur. Biophys. J.* 38, 305–318 [PubMed: 18449536]

9. Enyedi P., Czirják G. (2010) Molecular background of leak K^+ currents. Two-pore domain potassium channels. *Physiol. Rev.* 90, 559–605 [PubMed: 20393194]

10. Kim D. (2005) Physiology and pharmacology of two-pore domain potassium channels. *Curr. Pharm. Des.* 11, 2717–2736 [PubMed: 16101451]

11. Maingret F., Patel A. J., Lazdunski M., Honoré E. (2001) The endocannabinoid anandamide is a direct and selective blocker of the background K^+ channel TASK-1. *EMBO J.* 20, 47–54 [PMCID: PMC140203] [PubMed: 11226154]

12. Donner B. C., Schullenberg M., Geduldig N., Hüning A., Mersmann J., Zacharowski K., Kovacevic A., Decking U., Aller M. I., Schmidt K. G. (2011) Functional role of TASK-1 in the heart: studies in TASK-1-deficient mice show prolonged cardiac repolarization and reduced heart rate variability. *Basic Res. Cardiol.* 106, 75–87 [PubMed: 20978771]

13. Decher N., Wemhöner K., Rinné S., Netter M. F., Zuzarte M., Aller M. I., Kaufmann S. G., Li X. T., Meuth S. G., Daut J., Sachse F. B., Maier S. K. (2011) Knock-out of the potassium channel TASK-1 leads to a prolonged QT interval and a disturbed QRS complex. *Cell. Physiol. Biochem.* 28, 77–86 [PubMed: 21865850]

14. Limberg S. H., Netter M. F., Rolfes C., Rinné S., Schlichthörl G., Zuzarte M., Vassiliou T., Moosdorf R., Wulf H., Daut J., Sachse F. B., Decher N. (2011) TASK-1 channels may modulate action potential duration of human atrial cardiomyocytes. *Cell. Physiol. Biochem.* 28, 613–624 [PMCID: PMC3709183] [PubMed: 22178873]

15. Ishii Y., Schuessler R. B., Gaynor S. L., Yamada K., Fu A. S., Boineau J. P., Damiano R. J., Jr. (2005) Inflammation of atrium after cardiac surgery is associated with inhomogeneity of atrial conduction and atrial fibrillation. *Circulation* 111, 2881–2888 [PubMed: 15927979]

16. Bradley P. P., Priebat D. A., Christensen R. D., Rothstein G. (1982) Measurement of cutaneous inflammation. Estimation of neutrophil content with an enzyme marker. *J. Invest. Dermatol.* 78, 206–209 [PubMed: 6276474]

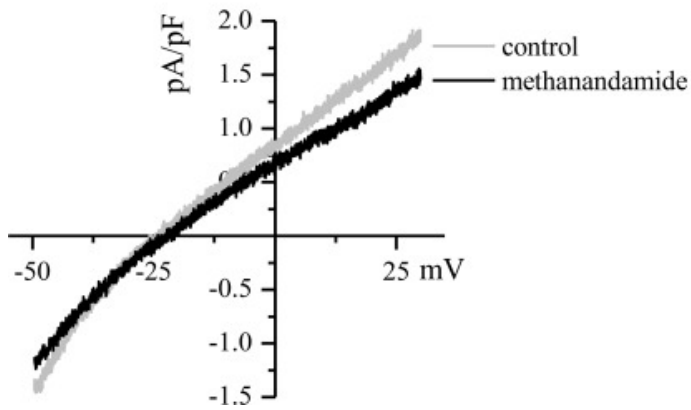
17. Peterson G. L. (1977) A simplification of the protein assay method of Lowry *et al.* which is more generally applicable. *Anal. Biochem.* 83, 346–356 [PubMed: 603028]
18. Johnson J. A., Gray M. O., Chen C. H., Mochly-Rosen D. (1996) A protein kinase C translocation inhibitor as an isozyme-selective antagonist of cardiac function. *J. Biol. Chem.* 271, 24962–24966 [PubMed: 8798776]
19. Ravens U., Cerbai E. (2008) Role of potassium currents in cardiac arrhythmias. *Europace* 10, 1133–1137 [PubMed: 18653669]
20. Nattel S. (2009) Calcium-activated potassium current. A novel ion channel candidate in atrial fibrillation. *J. Physiol.* 587, 1385–1386 [PMCID: PMC2678214] [PubMed: 19336611]
21. Ehrlich J. R., Zicha S., Coutu P., Hébert T. E., Nattel S. (2005) Atrial fibrillation-associated minK38G/S polymorphism modulates delayed rectifier current and membrane localization. *Cardiovasc. Res.* 67, 520–528 [PubMed: 16039273]
22. Li N., Timofeyev V., Tuteja D., Xu D., Lu L., Zhang Q., Zhang Z., Singapuri A., Albert T. R., Rajagopal A. V., Bond C. T., Periasamy M., Adelman J., Chiamvimonvat N. (2009) Ablation of a Ca^{2+} -activated K^+ channel (SK2 channel) results in action potential prolongation in atrial myocytes and atrial fibrillation. *J. Physiol.* 587, 1087–1100 [PMCID: PMC2673777] [PubMed: 19139040]
23. Putzke C., Wemhöner K., Sachse F. B., Rinné S., Schlichthörl G., Li X. T., Jaé L., Eckhardt I., Wischmeyer E., Wulf H., Preisig-Müller R., Daut J., Decher N. (2007) The acid-sensitive potassium channel TASK-1 in rat cardiac muscle. *Cardiovasc. Res.* 75, 59–68 [PubMed: 17389142]
24. Morillo C. A., Klein G. J., Jones D. L., Guiraudon C. M. (1995) Chronic rapid atrial pacing. Structural, functional, and electrophysiological characteristics of a new model of sustained atrial fibrillation. *Circulation* 91, 1588–1595 [PubMed: 7867201]
25. Gaspo R., Sun H., Fareh S., Levi M., Yue L., Allen B. G., Hebert T. E., Nattel S. (1999) Dihydropyridine and β -adrenergic receptor binding in dogs with tachycardia-induced atrial fibrillation. *Cardiovasc. Res.* 42, 434–442 [PubMed: 10533579]
26. Patel A. J., Honoré E., Lesage F., Fink M., Romey G., Lazdunski M. (1999) Inhalational anesthetics activate two-pore-domain background K^+ channels. *Nat. Neurosci.* 2, 422–426 [PubMed: 10321245]
27. Freeman L. C., Ack J. A., Fligner M. A., Muir W. W., 3rd (1990) Atrial fibrillation in halothane- and isoflurane-anesthetized dogs. *Am. J. Vet. Res.* 51, 174–177 [PubMed: 2301817]
28. Montrucchio G., Alloatti G., Camussi G. (2000) Role of platelet-activating factor in cardiovascular pathophysiology. *Physiol. Rev.* 80, 1669–1699 [PubMed: 11015622]
29. Baker K. E., Curtis M. J. (2004) Left regional cardiac perfusion *in vitro* with platelet-activating factor, norepinephrine, and K^+ reveals that ischaemic arrhythmias are caused by independent effects of endogenous “mediators” facilitated by interactions and moderated by paradoxical antagonism. *Br. J. Pharmacol.* 142, 352–366 [PMCID: PMC1574949] [PubMed: 15066909]
30. Flores N. A., Sheridan D. J. (1990) Electrophysiological and arrhythmogenic effects of platelet activating factor during normal perfusion, myocardial ischaemia, and reperfusion in the guinea pig. *Br. J. Pharmacol.* 101, 734–738 [PMCID: PMC1917725] [PubMed: 2076489]
31. Ishii S., Shimizu T. (2000) Platelet-activating factor (PAF) receptor and genetically engineered PAF receptor mutant mice. *Prog. Lipid Res.* 39, 41–82 [PubMed: 10729607]

32. Stangl V., Baumann G., Stangl K., Felix S. B. (2002) Negative inotropic mediators released from the heart after myocardial ischaemia-reperfusion. *Cardiovasc. Res.* 53, 12–30 [PubMed: 11744010]
33. Baker K. E., Curtis M. J. (1999) Protection against ventricular fibrillation by the PAF antagonist, BN-50739, involves an ischaemia-selective mechanism. *J. Cardiovasc. Pharmacol.* 34, 394–401 [PubMed: 10470998]
34. Qayumi A. K., English J. C., Godin D. V., Ansley D. M., Loucks E. B., Lee J. U., Kim C. W. (1998) The role of platelet-activating factor in regional myocardial ischemia-reperfusion injury. *Ann. Thorac. Surg.* 65, 1690–1697 [PubMed: 9647083]
35. Chakrabarty S., Fluck D. S., Flores N. A., Sheridan D. J. (1992) Effects of the PAF antagonists BN50726 and BN50739 on arrhythmogenesis and extent of necrosis during myocardial ischaemia/reperfusion in rabbits. *Br. J. Pharmacol.* 107, 705–709 [PMCID: PMC1907739] [PubMed: 1472967]
36. Baker K. E., Wood L. M., Whittaker M., Curtis M. J. (2006) Nupafant, a PAF-antagonist prototype for suppression of ventricular fibrillation without liability for QT prolongation? *Br. J. Pharmacol.* 149, 269–276 [PMCID: PMC2014274] [PubMed: 16921398]

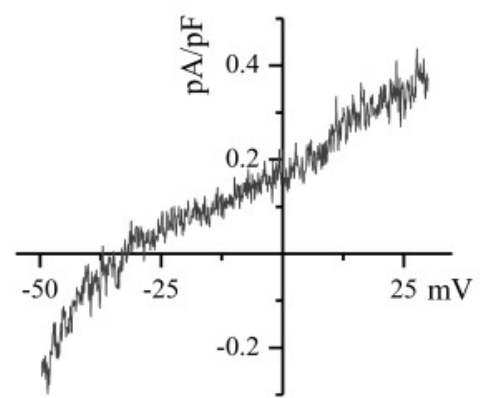
Figures and Tables

FIGURE 1.

A. Total Current

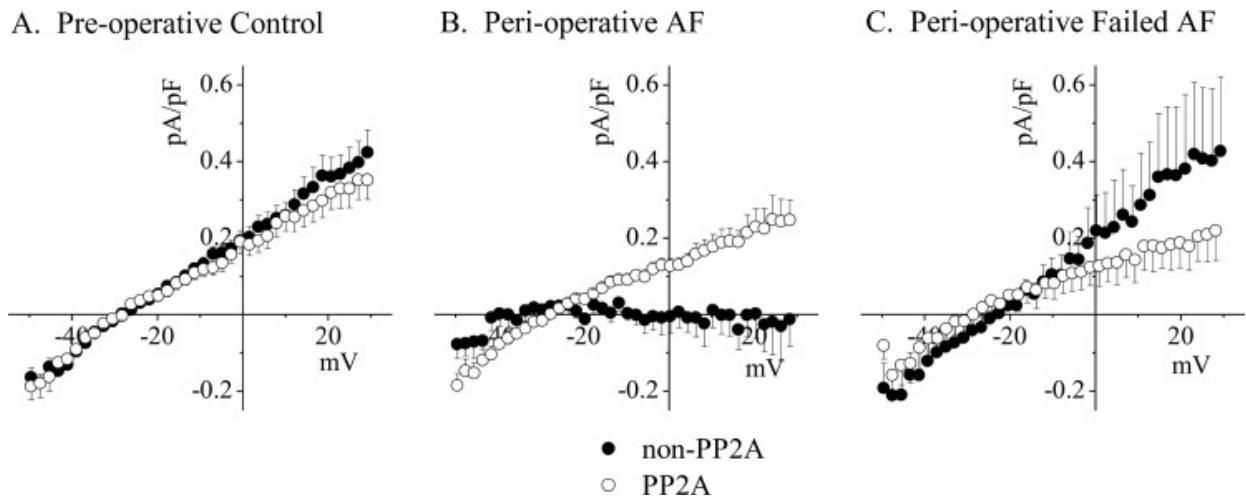


B. Methanandamide-Sensitive Current



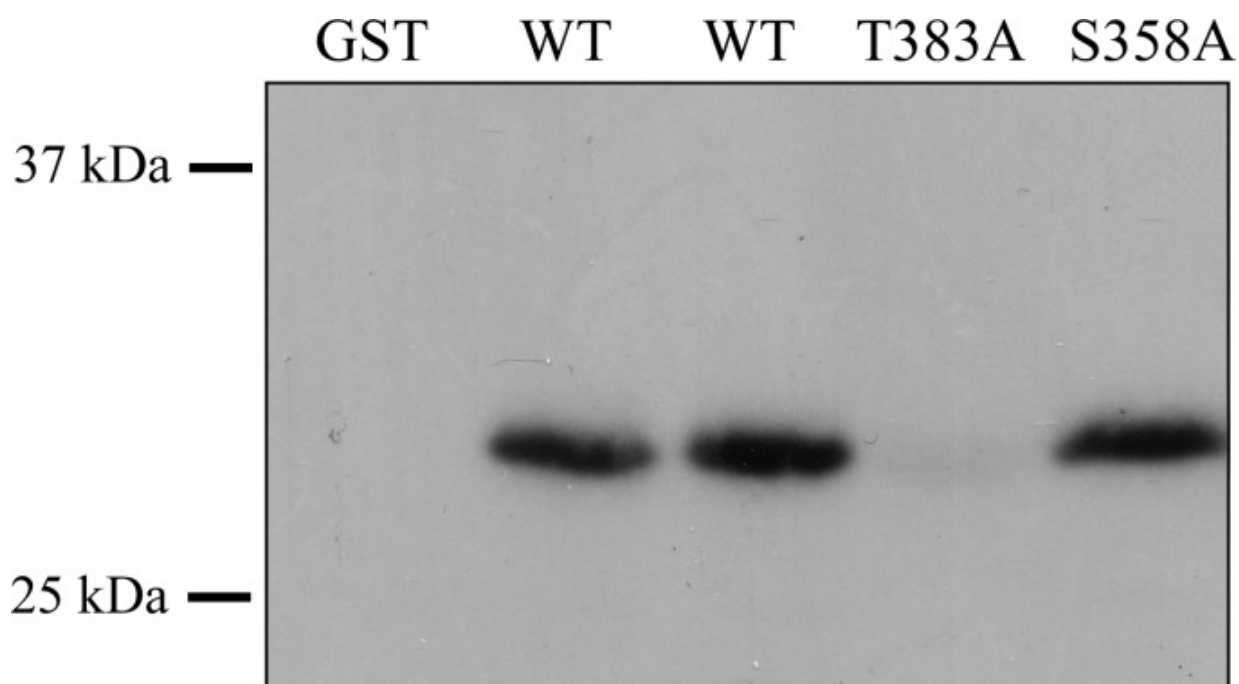
TASK-1 is measured as the methanandamide-sensitive difference current in isolated atrial myocytes. Canine myocytes were isolated from the right atrial free wall at the time of atriotomy, and whole cell currents were measured by patch clamp recording using a ramp protocol from -50 to $+30$ mV. The cells were bathed in elevated external K^+ (50 mM) to increase the inward component of the current and linearize the I/V curve and in the presence of CsCl (5 mM), TEA (2 mM), and nifedipine (5 μ M) to block other endogenous currents. *A* depicts a typical trace from a canine right atrial myocyte showing the total current measured from before and after the addition of methanandamide (10 μ M) to the superfusion. *B* depicts the methanandamide-sensitive difference current from the traces in *A*. The difference current is assumed to be TASK-1, and it displays the expected current-voltage relation and reversal potential consistent with a K_{2P} channel.

FIGURE 2.



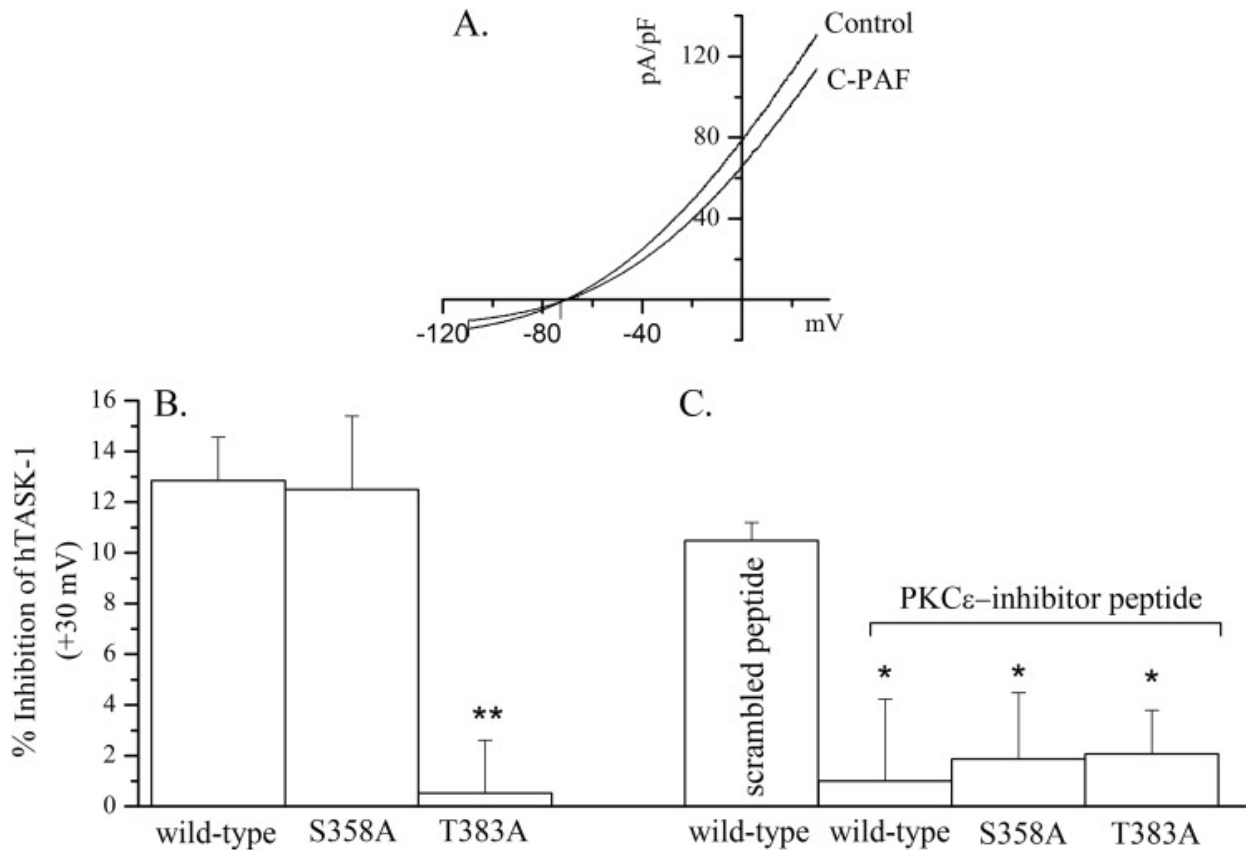
TASK-1 current is inhibited in a phosphorylation-dependent manner in myocytes from dogs with peri-operative AF. Myocytes were isolated from canine atrial myocardium at the time of atriotomy and after induction or failed induction of peri-operative AF. The methanandamide-sensitive TASK-1 current was measured by patch clamp recordings, and the average current density was plotted for pre-operative control (*A*, *filled circles*; $n = 52$ cells from 21 dogs), for peri-operative AF (*B*, *filled circles*; $n = 19$ cells from seven dogs), and for failed AF (*C*, *filled circles*; $n = 12$ cells from four dogs). Note that the TASK-1 current is absent from cells isolated after induction of peri-operative AF; however, addition of PP2A to the patch pipette rescued the current in cells isolated from the peri-operative AF dogs (*B*, *open circles*; $n = 16$ cells from seven dogs). PP2A caused no change in the current densities measured in cells from pre-operative control tissue (*A*, *open circles*; $n = 50$ cells from 20 dogs) or from dogs with failed AF induction (*C*, *open circles*; $n = 5$ cells from two dogs). The PP2A-rescued TASK-1 current density was not different from the current measured in cells from pre-operative control tissue ($p > 0.05$). Data are mean values \pm S.E.

FIGURE 3.



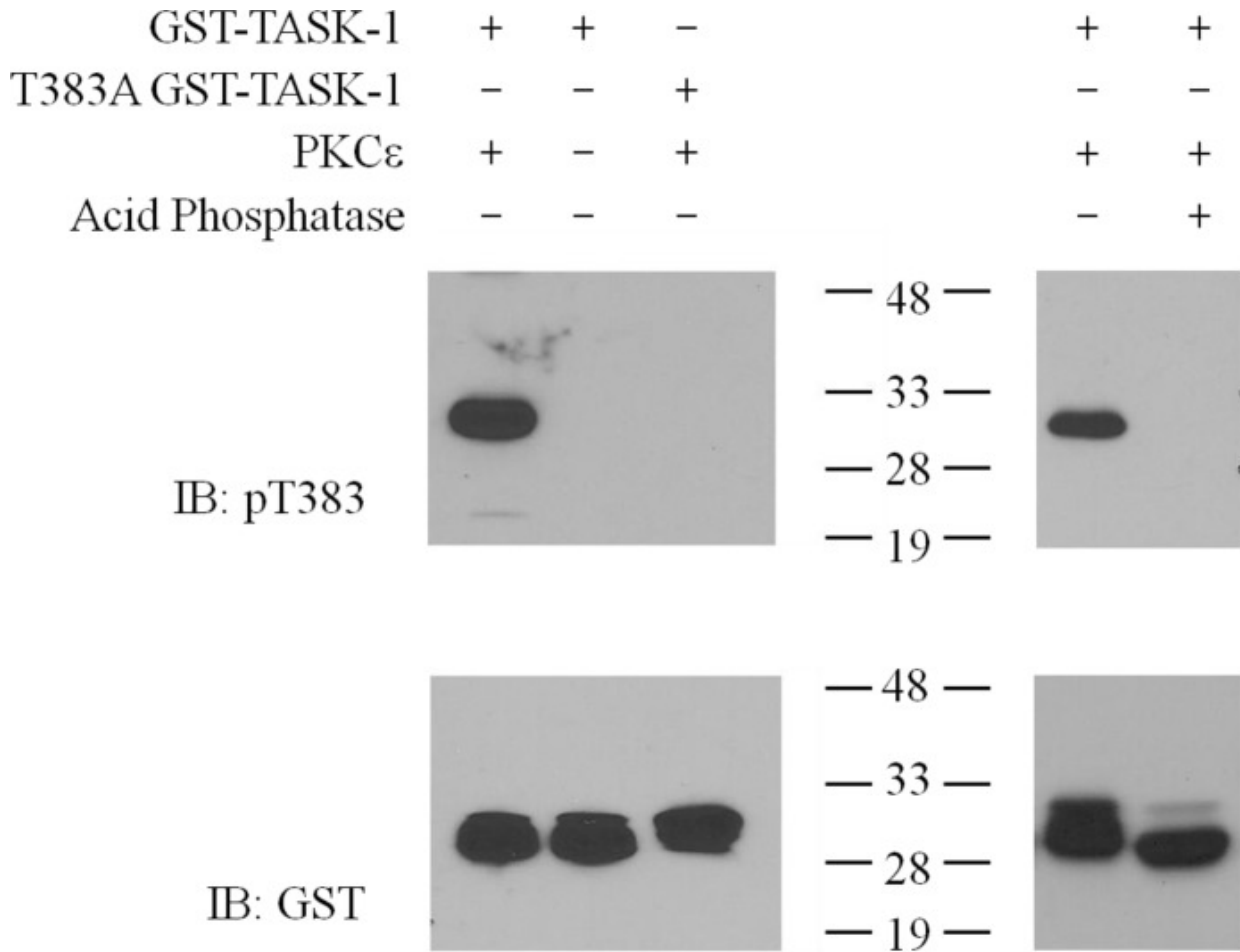
Threonine 383 is necessary for PKC ϵ phosphorylation of hTASK-1. The distal 45 residues of hTASK-1 were fused to GST, purified, and exposed to recombinant PKC ϵ in the presence of [γ - 32 P]ATP. Additional constructs were created that contained mutations of the putative phosphorylation sites in the channel. These constructs were also incubated with the kinase. The reaction products were resolved by SDS-PAGE, blotted to nitrocellulose, and analyzed by exposure to x-ray film. The presence of radioactivity in the bands indicates the incorporation of 32 P, and the result indicates that Thr-383 was required for phosphorylation by PKC ϵ .

FIGURE 4.



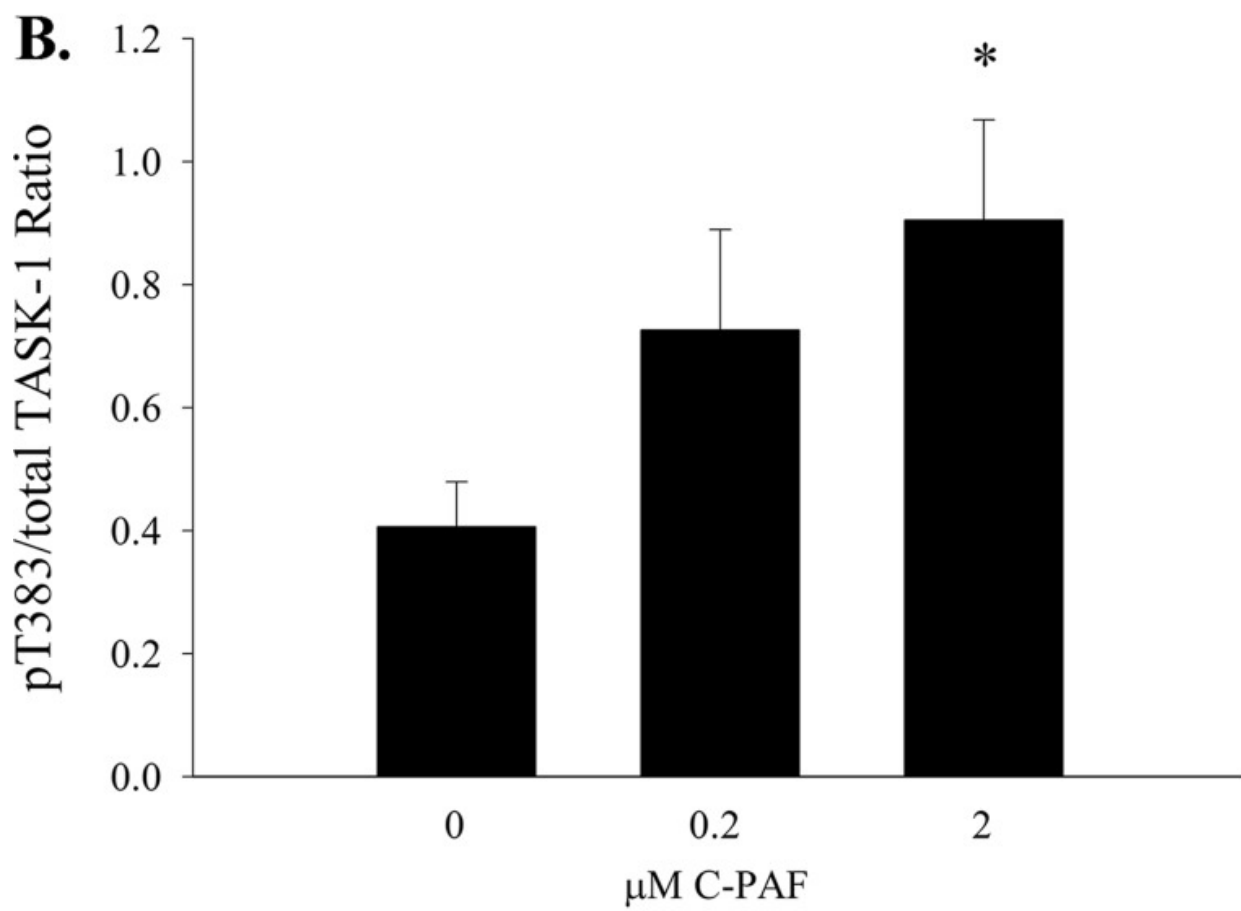
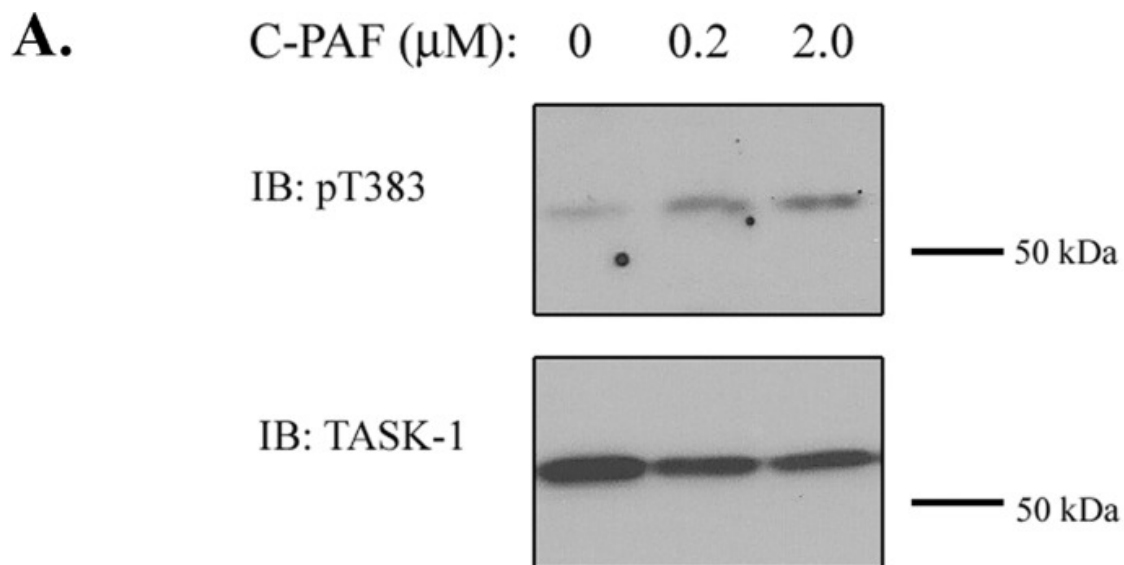
PKC ϵ -dependent inhibition of TASK-1 by C-PAF is abrogated by mutation of threonine 383 to alanine. Human TASK-1 was expressed in CHO cells, and the C-PAF-sensitive current was calculated from patch clamp recordings in the presence or absence of C-PAF (187 nM). *A* depicts a typical current-voltage relation for TASK-1 current under control conditions and in the presence of C-PAF. *B*, two TASK-1 mutants (S358A and T383A) were generated by site-directed mutagenesis and expressed in CHO cells, and the resulting currents were measured by patch clamp recording. The mean current value (\pm S.E.) at +30 mV was calculated for each construct. Mutation of serine 358 ($n = 11$) had no effect on the C-PAF-dependent inhibition of current compared with wild type ($n = 9$), whereas the C-PAF-dependent inhibition of the threonine mutant ($n = 14$) was significantly less than both wild type and S358A (**, $p < 0.01$). *C*, PKC ϵ -specific inhibitory peptide (or a scrambled control peptide) was dialyzed into the cells through the patch pipette, and then the inhibition of TASK-1 current was measured in the presence or absence of C-PAF. The control peptide had no effect on the C-PAF-sensitive TASK-1 current. In contrast, inhibition of PKC ϵ significantly reduced the C-PAF-dependent inhibition in all previously responsive constructs (*, $p < 0.05$).

FIGURE 5.



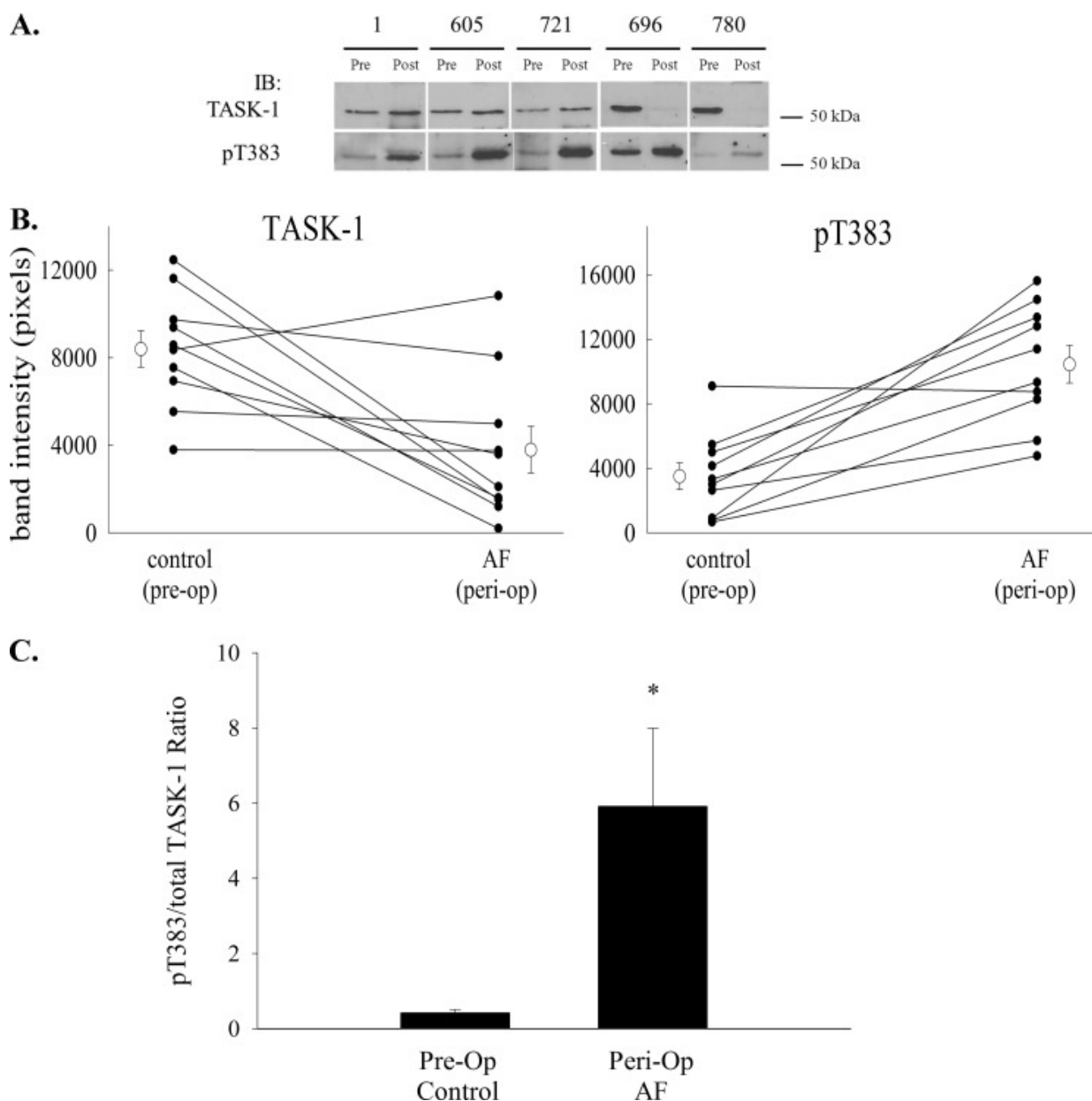
Thr(P)-383 phosphorylation site-specific antibody recognizes PKC ϵ -phosphorylated but not nonphosphorylated or dephosphorylated hTASK-1 C terminus fused to GST. Western blot analysis of *in vitro* kinase reactions of WT or Thr-383A hTASK-1 C terminus fused to GST that were phosphorylated (*1st* and *4th* lanes) or not phosphorylated (*2nd* lane) by PKC ϵ (*left panel*). Some reactions were subsequently dephosphorylated by acid phosphatase (*5th* lane, *right panel*). Proteins were resolved by SDS-PAGE and transferred to nitrocellulose. Phosphorylated Thr-383 was detected by immunoreactivity with a phosphorylation site-specific antibody (*top panel*), and total protein loading was confirmed by immunoreactivity with an anti-GST antibody (*bottom panel*). The Thr(P)-383 antibody is specific for the phosphorylated C terminus (*1st* and *4th* lanes), and it does not recognize protein that was not exposed to PKC ϵ (*2nd* lane), protein where the Thr-383 phosphorylation site was mutated (*3rd* lane), or protein that was dephosphorylated (*5th* lane). *IB*, immunoblot.

FIGURE 6.



C-PAF treatment of normal canine right atrial tissue increases the phosphorylation of TASK-1 at Thr-383. Normal canine right atrium was incubated with C-PAF (0–2 μM) for 15 min, after which crude membrane fractions of the homogenized tissue were prepared and analyzed by Western blotting for the presence of total TASK-1 and Thr(P)-383 TASK-1. *A* depicts a representative blot of Thr(P)-383 (*top panel*) and total TASK-1 (*bottom panel*) isolated from C-PAF-treated atrial myocardium. *B* depicts the summary of data from six experiments. C-PAF treatment resulted in a significant increase in Thr(P)-383 relative to total TASK-1 (*, $p < 0.05$, 2 μM versus 0 μM ; repeated measures analysis of variance). *C* depicts the summary of data from six independent experiments that included the addition of the PKC inhibitor BIM-1 (5 μM). Inhibition of PKC significantly reduced the C-PAF-dependent phosphorylation of Thr-383 (**, $p < 0.01$, 2 μM versus 0 μM or versus 2 μM + BIM-1; repeated measures analysis of variance). *IB*, immunoblot.

FIGURE 7.



Phosphorylation of TASK-1 at Thr-383 increases after the induction of peri-operative AF. Right atrial tissue was taken from dogs at the time of atriotomy and after induction of peri-op AF, and crude membrane fractions were prepared. Proteins were resolved by SDS-PAGE and blotted to nitrocellulose. Western blotting was used to quantify total TASK-1 and Thr(P)-383 TASK-1. *A* depicts several representative Western blots from tissue taken from five dogs before (*Pre*) or after (*Post*) induction of peri-op AF and immunoblotted for total TASK-1 (*left panel*) or Thr(P)-383 TASK-1 (*right panel*). *IB*, immunoblot. *B* depicts line graphs for each dog demonstrating the change in total TASK-1 (*top panel*) and Thr(P)-383 TASK-1 (*bottom panel*) before and after induction of peri-op AF. The mean (\pm S.E.) for all dogs is also depicted on the graph. *C*, relative fraction of TASK-1 phosphorylated at Thr-383 before and after peri-op AF was calculated and expressed as the ratio of Thr(P)-383 to total TASK-1. The induction of peri-op AF was associated with a significant increase in the Thr(P)-383/TASK-1 ratio ($n = 10$; *, $p < 0.05$, paired t test).